

Probing the Upper Limit of Nonclassical Rotational Inertia in Solid Helium 4

Ann Sophie C. Rittner* and John D. Reppy

Laboratory of Atomic and Solid State Physics and the Cornell Center for Materials Research, Cornell University,
Ithaca, New York 14853-2501

(Received 13 July 2008; published 9 October 2008)

We study the effect of confinement on solid ^4He 's nonclassical rotational inertia fraction (NCRIF) in a torsional oscillator by constraining it to narrow annular cells of various widths. The NCRIF exhibits an observed maximum value of 20% for annuli of $\sim 100\ \mu\text{m}$ width. Samples constrained to porous media or to larger geometries both have smaller NCRIF, mostly below $\sim 1\%$. In addition, we extend the blocked-annulus experiment of Kim and Chan to solid samples with large supersolid fractions. Blocking the annulus suppresses the nonclassical decoupling from 17.1% to below the limit of our detection of 0.8%. This result demonstrates the nonlocal nature of the supersolid phenomena. At 20 mK, NCRIF depends on velocity history showing a closed hysteresis loop in different thin annular cells.

DOI: 10.1103/PhysRevLett.101.155301

PACS numbers: 67.80.bd, 66.30.Ma

Kim and Chan (KC) have observed an anomalous decrease in solid ^4He 's rotational inertia below 200 mK in a torsional oscillator [1,2]. The possibility of a new "super" state of matter sparked a flurry of experimental and theoretical work. When an annular cell is blocked, the nonclassical rotational inertia fraction (NCRIF) is strongly reduced [2], indicating that superflow is responsible for the nonclassical rotational inertia (NCRI). To date, the blocked-annulus experiment is the strongest experimental evidence supporting superflow over other explanations such as the unusual temperature dependence of the elastic properties of the solid [2]. Further support for superflow is that the oscillation frequency seems to have no impact on the signal size [3]. NCRI has been confirmed in several laboratories [4,5] with supersolid fractions ranging from 0.03% up to 20% [6]. The supersolid fraction can be altered by experimental parameters such as ^3He impurity concentration [1], thermal history of the sample [5], sample pressure, and geometric confinement [6]. Notably, the supersolid fraction increases by more than 3 orders of magnitude when thin annular geometries confine the sample. There has been a growing consensus that crystalline defects are crucial to enhance NCRIFs (for a review see [7]). Microscopic models suggest the involvement of grain boundaries [8], dislocation networks [9], a superglass phase [10], or a dislocation glass [11].

The goals of our study are twofold: first, the sample confinement is increased below $150\ \mu\text{m}$ [6] to maximize the supersolid fraction. Second, we block annular cells with high NCRIFs to test if these samples also exhibit the characteristic superflow behavior seen by KC.

We observe maximum NCRIF $\sim 20\%$ in narrow annuli of $\sim 100\ \mu\text{m}$. In a narrow annular cell, we confirm the blocked-annulus result [2]: inserting a block in the flow path suppresses the supersolid fraction from 17.1% to below our experimental resolution of 0.8%.

In our latest design, we have constructed the torsion rod and the body of the torsional oscillator from the aluminum

alloy 6061T6. Figure 1 shows our aluminum torsional oscillator with an annular geometry. Its resonance frequency is 484.1 Hz at temperature $T = 4\ \text{K}$ with a quality factor, Q , of 5.3×10^5 when the rods are in place. The inner wall and torsion rod are made out of one piece to minimize the relative motion of the two constraining walls of the annulus. This design lessens the impact on the resonance period from ^4He shear modulus changes [12].

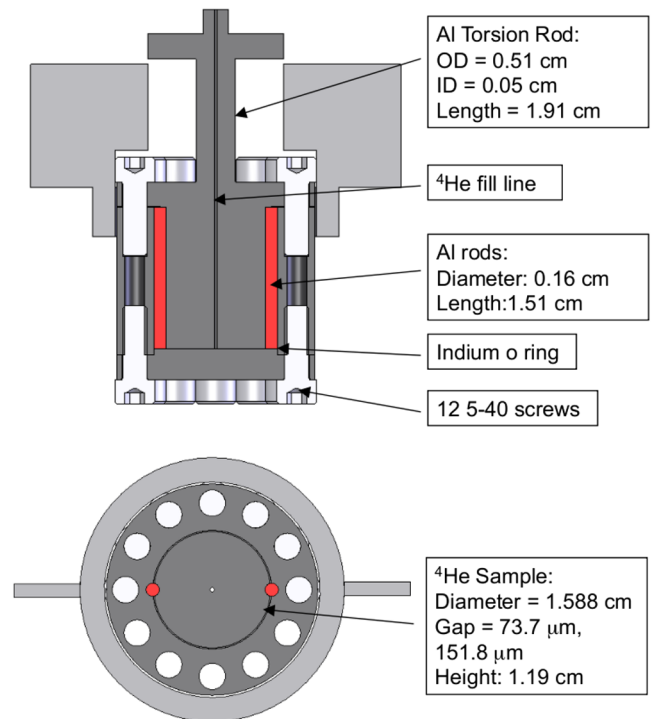


FIG. 1 (color online). Aluminum torsional oscillator with removable blocks (in red). The thin annular gap widths of 73.4 and $148.3\ \mu\text{m}$ resulted in mass loading of 45.5 and $91.9\ \text{ns}$, respectively. At 20 mK, the resonance frequency is 484.1 Hz and the quality factor of the oscillation is $Q \sim 5.3 \times 10^5$ when the rods are in place.

Another unique feature of our oscillator is that we can reversibly block it by introducing two rods that are centered in the annulus (diameter = 1.59 mm, shown in red in Fig. 1). This allows us to repeat KC's blocked-annulus experiment [2] in thin cells with large supersolid fractions. The blocks also provide a means to measure the moment of inertia of the solid, which is needed to compute supersolid fractions from the observed period drops. There are three configurations for the oscillator: first the blocked configuration with rods sealed in place; second, with slightly smaller diameter rods to maintain an annulus of constant width; and third with the rods absent, to study the effect on the NCRIF of a larger region in the path of the superflow. We employ annuli with two different spacings, 148.3 and 73.4 μm with surface to volume ratios (S/V) of 134.8, and 272.5 cm^{-1} , respectively.

In most supersolid experiments, the total moment of inertia of the solid is determined by the period increase upon freezing. In small volume cells such as our narrow annuli, this increase is obscured by a simultaneous decrease due to the dropping pressure. In our experiment, a typical pressure drop of 30 bar in the cell during solidification results in a period drop of 60 ns. For the 73.4 μm cell, this drop exceeds the 45.5 ns period rise from solidification, making it impossible to use the standard experimental method. Alternatively, we can determine the solid inertia in our small volume cells by blocking the annulus: since the fluid backflow is negligible in thin annuli, a block in the flow locks the bulk liquid in the oscillator. When liquid enters the cell, two effects cause the resonance period to increase: the additional inertia stemming from the liquid ^4He as well as the cell's expansion due to the pressure. To separate pressure effects from the period change due to coupling of the liquid, we measure the resonance period as a function of liquid pressure in the cell. The extrapolation of the period to zero pressure is shifted with respect to the zero pressure measured period before the cell was filled. This period offset, ΔP , is the period change that stems from filling the cell with liquid at zero pressure. In order to calculate the period shift due to solid helium ΔP is rescaled by the ratio of solid density, depending on pressure $\sim 0.2 \text{ g/cm}^3$, to liquid density. The solid mass loadings in the 73.4 and 148.3 μm cells are 45.5 and 91.9 ns, respectively. All supersolid fractions are calculated by dividing the NCRIF period drop by the solid mass loading.

We also use liquid ^3He in calibrating our cell. Here, we take advantage of the strong temperature dependence of the viscosity of liquid ^3He [13]. Above 100 mK, the viscosity is low and the fluid is mostly decoupled from the motion of the torsion bob. As the temperature is lowered, the viscosity increases and the fluid locks in the annulus. The total fluid inertia can be determined from temperature and height of the dissipation maximum and from the period shift upon locking the liquid. The mass

loadings determined with the viscosity of liquid ^3He and liquid ^4He in the blocked annulus differ by less than 5%.

Figure 2 displays our main result of this series of experiments; the supersolid fractions are shown as a function of S/V in different cells. In thin annular cells with gap, t , S/V simplifies to $\frac{2}{t}$. For large open geometries, the supersolid fraction is small, 0.03%. As we have reported before, the signal size increases dramatically by 3 orders of magnitude [6] with stronger confinement. In our latest data (solid stars), we find that the maximum signals observed are around 20% at $S/V \sim 150 \text{ cm}^{-1}$. When the sample is constrained further [14,15] the NCRIF decreases back to $\approx 1\%$ for $S/V \sim 10^5 \text{ cm}^{-1}$. Contrary to previous attempts in larger cells [5,6], quench-cooling or annealing (typically at $\sim 1.7 \text{ K}$ for $\sim 6 \text{ h}$) fail to alter the signal size in this series of narrow annular oscillators.

Important information may be extracted from the maximum observed NCRIF and the length scale at which it occurs. First, the maximum NCRIF rules out the explanation of superflow by a network of grain boundaries as 20% NCRIF would require a grain size of a few \AA [16]. A less simple theory involving grain boundaries might be reconciled with our observations.

Similarly, the maximum NCRIF is difficult to reconcile with a dislocation network with superfluid cores. The measured dislocation density in a sample space with $S/V = 2 \text{ cm}^{-1}$ [17] is consistent with the expected supersolid signal of 0.1% in a similar geometry assuming a superfluid core of 6 \AA [10]. On the other hand, a supersolid fraction, ρ_s/ρ , of 20% would require a dislocation density

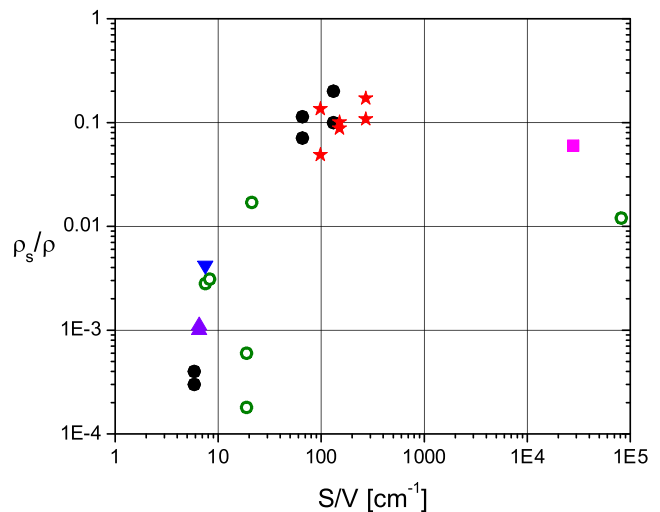


FIG. 2 (color online). The supersolid fraction, ρ_s/ρ , plotted as a function of the surface to volume ratio. The geometries from left to right are an open large cylinder (solid circles) [6], a cylinder (triangles) [3], two slightly different cylinders (open circles) [22], a cylinder (inverted triangle) [4], a welded annulus (open circles) [23], an annular cell (open circles) [2], thin annuli (solid circles and stars) [6], porous gold (square) [15], and smaller pore size gold (open circle) [14].

of 10^{13} cm^{-2} . This required density is 3 orders of magnitude higher than the highest measured dislocation density, corresponding to a spacing between dislocations of 3 nm. It is improbable that this simple model can fully explain the supersolid results.

In a model that better accounts for the NCRIF's geometry dependence, disorder is concentrated in a layer close to the walls [18]. This picture is consistent with the suggestion that dislocations form preferentially near cell walls in solid helium [19]. The surface roughness determines the penetration depth of the dislocation network, $\approx 1\text{--}5 \mu\text{m}$ for a polished metal surface. The maximal NCRIF is expected in an annular cell when the spacing is approximately twice the disordered layer thickness. Assuming that the supersolid fraction in the disordered region adjacent to the walls is 20%, we calculate the penetration depth to vary between 37 (current data) and $169 \mu\text{m}$ [6]. The penetration depth varies less between cells within the same series than between cells out of different materials. This larger variation may be related to different surface roughness. This simple model cannot easily explain the small NCRIF in porous media.

The second goal of our experiments is to check if the high apparent supersolid fractions can still be attributed to long range superflow. For this reason, we repeat KC's blocked-annulus experiment [2] in our narrow annular cells. In the blocked-annulus experiment, a partition is placed across the annular channel, thus interrupting any long range flow around the annulus. The basic idea is to

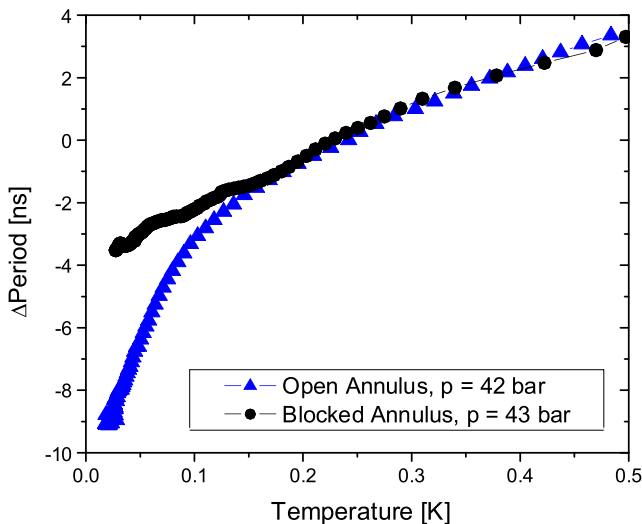


FIG. 3 (color online). Resonance period as a function of temperature in an unblocked (solid triangles) and blocked (solid circles) annulus with a width of $73.4 \mu\text{m}$. Both open and blocked-annulus data are taken in the same cell which could be reversibly blocked (see Fig. 1). The periods are adjusted to agree at 300 mK. The nonclassical rotational inertia decoupling is 17.1% of the solid inertia in the open annulus. For the blocked annulus, the upper limit to the NCRIF is 0.8% corresponding to a more than 20-fold reduction upon blocking.

compare the magnitude of supersolid signals in an open and in a blocked annulus of the same width. In the experiment performed to date, the solid helium moment of inertia decreases upon blocking, indicating that the macroscopically coherent supercurrent is suppressed. As a minor caveat, there remains a small contribution to the NCRIF from potential flow induced by the rotational motion of the oscillator. In the limit of a long narrow blocked channel, the NCRIF from this backflow becomes negligibly small compared to the NCRIF for the unimpeded flow in an unblocked channel. For example, in a 0.65 mm annulus, the period drop is reduced 200-fold [2]. Our annular width is $73.4 \mu\text{m}$, more than 10 times smaller than Kim and Chan's original cells (gap KC: open annulus = 0.95 mm , blocked annulus = 1.1 mm [16]) and the expected blocked-annulus NCRIF is below our resolution.

Figure 3 displays the resonance period as a function of temperature for both open and blocked annuli. Upon blocking the period drop at the supersolid transition is suppressed. Given the noise level of the experiment, the upper limit on a residual period drop in the blocked cell is $\sim 0.8\%$. The open cell displays a supersolid fraction of 17.1%, so the block suppresses the signal more than 20-fold. The major advantage of our setup with regard to KC's [2] is that our cell can be reversibly blocked, allowing one

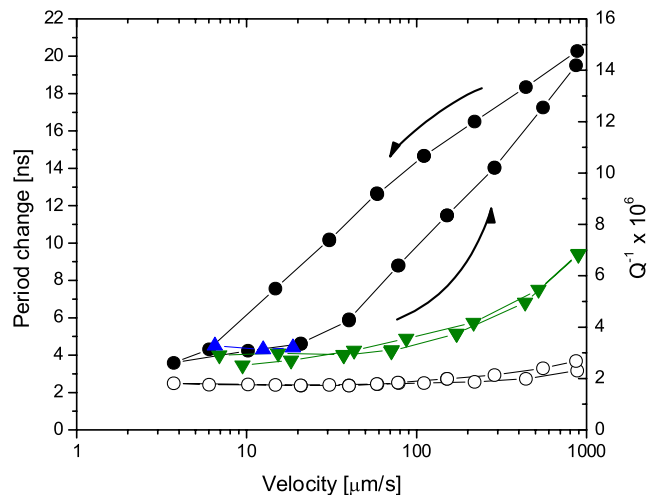


FIG. 4 (color online). Velocity dependence of resonance period difference (solid circles) and dissipation (open circles) at 20 mK in annular cell with a width of $148.3 \mu\text{m}$. First, the sample is cooled at a high velocity, $v = 881 \mu\text{m/s}$, to 20 mK and then the drive is reduced at constant temperature. After reaching a low velocity, $v = 3.8 \mu\text{m/s}$, the drive is increased again. The critical velocity in this cell is $\sim 20 \mu\text{m/s}$, as indicated by the low temperature period of cool downs at a constant drive level (triangles). We only show data points that were taken after the oscillator had time to equilibrate, about 20 min. Arrows indicate the direction of the velocity changes. For comparison, period difference data of the empty cell (inverted triangles) are displayed. Empty cell and solid helium period are shifted by 2.065582 ms and 2.065550 ms , respectively.

to measure open and blocked annuli within the same cell. We have also blocked a bigger annulus with a width of $487\ \mu\text{m}$ and find the upper limit for a remnant supersolid signal to be 0.4%. In the open geometry, we expect the NCRIF to be $\sim 5\%$ (see Fig. 2). Confirmation of the blocked-annulus result demonstrates the nonlocal nature of the supersolid phenomenon. Thus, local models, such as [20], are unlikely to provide a full explanation of the supersolid.

We have also studied the effect of removing the rods and thus interposing a larger volume in series with the superflow. Although the fractional signal is smaller, $\sim 6\%$, the total decoupled mass is similar in both configurations, $1.9 \times 10^{-5}\ \text{g}$ and $1.75 \times 10^{-5}\ \text{g}$ (without rods).

Finally, we have measured the velocity dependence of the supersolid fraction below 40 mK [3,16] in an annular cell with a $148.3\ \mu\text{m}$ gap. Figure 4 displays resonance period (solid circles) and dissipation (open circles) as a function of rim velocity, v , at 20 mK. The empty cell background (inverted triangles) is displayed for comparison. Following a similar experimental procedure as [3], we cool the sample to 20 mK while oscillating at a high rim velocity, $v = 881\ \mu\text{m/s}$. Holding the temperature fixed, the velocity is decreased in steps and then held for ~ 20 min until amplitude and period equilibrate as determined by the oscillator's Q . Holding the drive constant for up to 3 h does not alter period and amplitude further. Starting from the lowest velocity $v = 3.8\ \mu\text{m/s}$, we raise the velocity in steps. When the velocity surpasses $\sim 20\ \mu\text{m/s}$, the period rises more steeply than the empty cell period, indicating that this cell's critical velocity has been exceeded. The period difference between cell filled with solid helium and empty cell at the highest velocity corresponds to a supersolid fraction of 12.0%. We observe some hysteresis between decreasing and increasing velocity, that is, the resonance period depends on the velocity history. In contrast, the resonance period shows no hysteresis at 60 and 200 mK.

Our finding differs from Aoki *et al.*'s observations in a cylindrical cell [3]. When their sample velocity increases, the NCRIF stays constant above the critical velocity of 15, up to $800\ \mu\text{m/s}$. Also in a cylindrical cell, Clark *et al.* [16] find a correlation between the sample growth method and the NCRIF stability when the velocity is increased: constant pressure grown samples with relatively low NCRIF are metastable at low temperatures, while the NCRIF of blocked capillary grown samples is unstable against an increase in velocity. They attribute the existence of metastable states to severe vortex pinning in the sample at low temperatures, in qualitative agreement with Anderson's vortex liquid model [21]. The major difference between our experiments and other groups' lie in the annular geometry, stronger confinement and much higher supersolid fractions. Possibly, the smaller hysteresis in confined geometries can be attributed to the fact that vortices cross the

sample more easily, for example, because of a lower density of pinning centers.

In summary, we have increased the NCRIF to 20% by confining samples to narrow annular cells. Blocking a narrow annular cell strongly reduces the NCRIF which is consistent for superflow.

We thank M. Chan, J. West, A. Clark, X. Lin, E. Kim, and E. Mueller for information about their torsional oscillators and discussions, and we thank K. Hazzard for a critical reading of the manuscript. This work has been supported by the National Science Foundation under Grant DMR-060584 and through the Cornell Center for Materials Research under Grant DMR-0520404.

*ar297@cornell.edu

- [1] E. Kim and M. Chan, *Nature (London)* **427**, 225 (2004).
- [2] E. Kim and M. Chan, *Science* **305**, 1941 (2004).
- [3] Y. Aoki, J. C. Graves, and H. Kojima, *Phys. Rev. Lett.* **99**, 015301 (2007).
- [4] M. Kondo, S. Takada, Y. Shibayama, and K. Shirahama, *J. Low Temp. Phys.* **148**, 695 (2007).
- [5] A. S. C. Rittner and J. D. Reppy, *Phys. Rev. Lett.* **97**, 165301 (2006).
- [6] A. S. C. Rittner and J. D. Reppy, *Phys. Rev. Lett.* **98**, 175302 (2007).
- [7] S. Balibar and F. Caupin, *J. Phys. Condens. Matter* **20**, 173201 (2008); N. V. Prokof'ev, *Adv. Phys.* **56**, 381 (2007).
- [8] L. Pollet, M. Boninsegni, A. B. Kuklov, N. V. Prokof'ev, B. V. Svistunov, and M. Troyer, *Phys. Rev. Lett.* **98**, 135301 (2007).
- [9] M. Boninsegni, A. B. Kuklov, L. Pollet, N. V. Prokof'ev, B. V. Svistunov, and M. Troyer, *Phys. Rev. Lett.* **99**, 035301 (2007).
- [10] M. Boninsegni, N. V. Prokof'ev, and B. V. Svistunov, *Phys. Rev. Lett.* **96**, 105301 (2006).
- [11] A. V. Balatsky, M. J. Graf, Z. Nussinov, and S. A. Trugman, *Phys. Rev. B* **75**, 094201 (2007).
- [12] J. Day and J. Beamish, *Nature (London)* **450**, 853 (2007).
- [13] J. M. Parpia, D. J. Sandiford, J. E. Berthold, and J. D. Reppy, *Phys. Rev. Lett.* **40**, 565 (1978).
- [14] E. Kim and M. H. W. Chan, *J. Low Temp. Phys.* **138**, 859 (2005).
- [15] E. Kim (private communication).
- [16] A. C. Clark, J. D. Maynard, and M. H. W. Chan, *Phys. Rev. B* **77**, 184513 (2008).
- [17] F. Tsuruoka and Y. Hiki, *Phys. Rev. B* **20**, 2702 (1979).
- [18] K. R. A. Hazzard (private communication).
- [19] Y. Kosevich and S. Svatko, *Fiz. Nizk. Temp.* **9**, 193 (1983).
- [20] A. Andreev, *JETP Lett.* **85**, 585 (2007).
- [21] P. W. Anderson, *Nature Phys.* **3**, 160 (2007).
- [22] A. C. Clark, J. T. West, and M. H. W. Chan, *Phys. Rev. Lett.* **99**, 135302 (2007).
- [23] J. T. West (private communication).